Core and valence level photoemission and photoabsorption study of icosahedral Al–Pd–Mn quasicrystals

2006 J. Phys.: Condens. Matter 18 435

(http://iopscience.iop.org/0953-8984/18/2/007)

INSTITUTE OF PHYSICS PUBLISHING JOURNAL OF PHYSICS: CONDENSED MATTER

J. Phys.: Condens. Matter **18** (2006) 435–448 doi:10.1088/0953-8984/18/2/007

Core and valence level photoemission and photoabsorption study of icosahedral Al–Pd–Mn quasicrystals

K Horn[1], W Theis[2], J J Paggel[2], S R Barman[3], E Rotenberg[4], Ph Ebert[5] and K Urban[5]

[1] Fritz-Haber-Institut der Max-Planck-Gesellschaft, Berlin, Germany
[2] Fachbereich Physik der Freien Universität Berlin, D-14195 Berlin, Germany
[3] UGC-DAE Consortium for Scientific Research, Indore, India
[4] Advanced Light Source, Lawrence Berkeley Laboratory, Berkeley, CA 94 720, USA
[5] Institut für Festkörperforschung, Forschungszentrum Jülich GmbH, D-52425 Jülich, Germany

Received 23 June 2005, in final form 20 October 2005
Published 14 December 2005
Online at stacks.iop.org/JPhysCM/18/435

Abstract

The electronic structure of quasicrystalline Al–Pd–Mn is investigated by means of valence and core level photoelectron spectroscopy. Variations of the photoionization cross section in the constituents' valence electronic levels as a function of photon energy are used to identify contributions from the different atomic species, in particular near the Pd 4d Cooper minimum. Resonant photoemission at the Mn 2p absorption edge shows the contribution of the Mn 3d states to the density of states in a region near the Fermi level. The asymmetry of Pd 3d and Mn 2p core level photoemission lines, and its difference for emission from metallic and quasicrystalline phases, are utilized to infer the contributions of the different constituents to the density of states at the Fermi level.

1. Introduction

In spite of more than a decade of intense research, the intriguing physical properties of quasicrystalline alloys, such as their extremely low electrical conductivities, unusual optical conductivities $\sigma(\omega)$, or low electronic contributions to the specific heat, still await explanation in terms of the characteristics of the valence level states [1–4]. In order to achieve such insight, it is necessary to adapt conventional notions used to describe the electronic structure in periodic solids to the unique order and symmetry of quasicrystals. For a detailed understanding of the electronic structure of solids, photoelectron spectroscopy has developed into an extremely useful tool [5, 6], and it has also been applied to quasicrystalline materials in recent years [4, 7–10]. Issues addressed in recent studies have been the evidence for the existence of a pseudogap [11, 12], the assignment of features in the valence level spectrum to the different constituent atoms [13] from cross-section considerations and resonant photoemission, and the

evidence for dispersing states in the valence level spectrum [14, 15]. Attention has also been paid to the variations in relative intensities in the valence level region, and the intensities and line shapes of core level emission [16].

Here we take up these issues in a core and valence level photoemission study from the fivefold surface of icosahedral (i) Al–Pd–Mn, from both cleaved and sputter-annealed surfaces. We distinguish contributions from each atomic species to the valence level region of the spectrum, and to the density of states at E_F in particular. These studies are based on differences in cross-section, which are accentuated by varying the kinetic energy of emission from specific levels. Another method employed is resonant photoemission from specific regions in the valence band, upon crossing an excitation threshold for a deep core level. Finally, we identify contributions to the region in the immediate vicinity of the Fermi level from the core level line shape. Core level lines in metallic systems have long been known to be asymmetric, having a tail towards the high binding energy side of the line, due to the screening of the core hole by electron–hole pair excitations across the Fermi level. This asymmetry depends, among other things, on the valence density of states of the core-ionized element. Thus a measurement of the asymmetry of core level lines from the different elements in an alloy may permit an identification of those elements which most strongly contribute to the density of states at E_F.

2. Experimental details

The experiments were carried out on beamline 7.0.1 at the Advanced Light Source, Lawrence Berkeley Laboratory, California. Photons from a 5 cm period undulator are dispersed by a spherical grating monochromator equipped with three grids covering the photon energy range from about 60 to 1200 eV, with a spectral resolution $\Delta E/E$ of about 3000–5000. The photoelectrons excited by the uv light are energy-analysed by an electrostatic hemispherical electron energy analyser (PHI model 10-360) and detected by a channelplate array. The i-$Al_{70.5}Pd_{21}Mn_{8.5}$ samples were grown in the Institut für Festkörperforschung of the Forschungszentrum Jülich. One set of data was recorded from samples cleaved in ultrahigh vacuum (base pressure 2×10^{-10} mbar) perpendicular to the fivefold axis. Another set of data was recorded from a pre-polished disc of i-$Al_{70.5}Pd_{21}Mn_{8.5}$ in the fivefold orientation, cleaned by neon ion sputtering and prolonged annealing at 800 K. Cleanliness of the samples was ascertained from an absence of an oxide shoulder on the Al 2p peak, recorded under conditions of extreme surface sensitivity, and the absence of other contaminants as identified from the entire photoelectron spectrum. Sample cleaning was repeated about every 2–3 h. This sputter-annealed sample exhibited a fivefold low-energy electron diffraction pattern [17], and a fivefold symmetry in the azimuthal intensity distribution of the Pd 3d and Al 2p Mn 2p core level lines, excited with Mg Kα radiation as reported in the literature [18], and used for a determination of its surface structure in photoelectron diffraction [19]. The surface was thus quasiperiodically well ordered.

3. Results and discussion

3.1. Photon energy dependence of the valence band spectral shape

An overview spectrum of a freshly cleaved i-Al–Pd–Mn quasicrystal is displayed in figure 1, recorded at a photon energy of 450 eV. The spectrum shows the dominant lines due to the Pd 3d, Al 2p, and valence band states. The region towards the low binding energy side of the Al 2p line contains additional structure, showing up as a progression of peaks. These are identified as plasmon peaks, superimposed on which is the sharp structure of the Al 2s line.

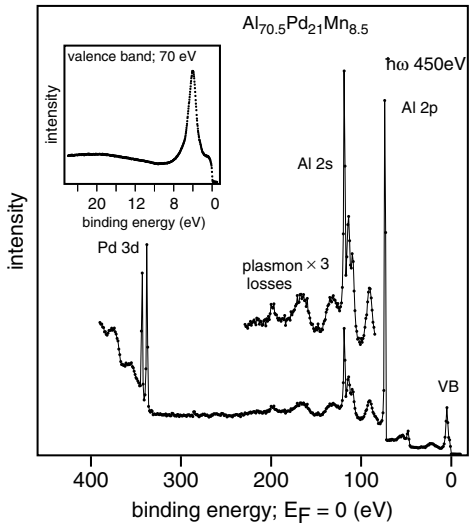

Figure 1. Overview spectrum of a freshly cleaved Al–Pd–Mn sample, recorded at a photon energy of 450 eV. Note the Al 2p and Pd 3d emission and the intense plasmon satellite lines on the high binding energy side of the Al 2p peak. The shape of the valence level spectrum, recorded at a photon energy of 70 eV, is shown in the inset.

Similar loss features are shown on the Pd 3d peak; their energy difference to the main line is about 17 eV, i.e. slightly larger than the bulk plasmon energy of the main constituent of Al–Pd–Mn, i.e. the Al bulk plasmon with an energy of 15.3 eV [20]. The Mn 3p level gives rise to the weak peaks at about 50 eV binding energy. The inset shows the valence level spectrum, recorded in normal emission at a photon energy of 70 eV, which is characterized by a strong peak centred around 4 eV below E_F, with a broad and smooth shape at higher binding energies, and a somewhat more intense emission directly at E_F. The peak at about 4 eV binding energy stems from the Pd 4d states [13]. Electrons in this level form a 'virtual bound state' since they are located within the region of the host Al s–p band and interact with this band, such that an electron in the d level can be scattered in and out of this level, making it only virtually bound [21]. The 4d states of Pd in i-Al–Pd–Mn are thus fully occupied, in contrast to Pd metal, where the 4d state emission extends up to the Fermi level. The intensity between the Pd-derived peak and the Fermi edge has been assigned to states with Mn 3d character [13], in agreement with x-ray emission spectra from i-Al–Pd–Mn [22] and calculations of the partial density of states (DOS) [23]. A breakdown of the valence level density of states into many very fine spikes, which is predicted from calculations (see, for example, the chapter by Hafner in [4]) is absent in the photoemission spectra. This is a general observation (e.g. [11, 13]) and not restricted to the case of Al–Pd–Mn. This obvious discrepancy, i.e. the absence of experimental evidence for a spiky density of states in photoemission data, was recently studied by Zijlstra and Janssen, who calculated the density of states in the vertex model of the Penrose tiling, and found that a surface can smoothen out the spikes [24]. Moreover, they calculated the density of states of the ideal three-dimensional Penrose tiling, and found that the latter does not exhibit spikes in the DOS [25], in contrast to the two-dimensional case where they occur. Zijlstra and Janssen relate the difference between their finding and earlier reports to an insufficient number of k-points in the evaluation of periodic approximants used.

The nominal occupation of the valence shell of the constituent atoms of Al–Pd–Mn is $[Ne]3s^2 3p^1$ for Al, $[Kr]4d^{10}5s^0$ for Pd, and $[Ar]3d^5 4s^2$ for Mn. The Pd 4d states have a node

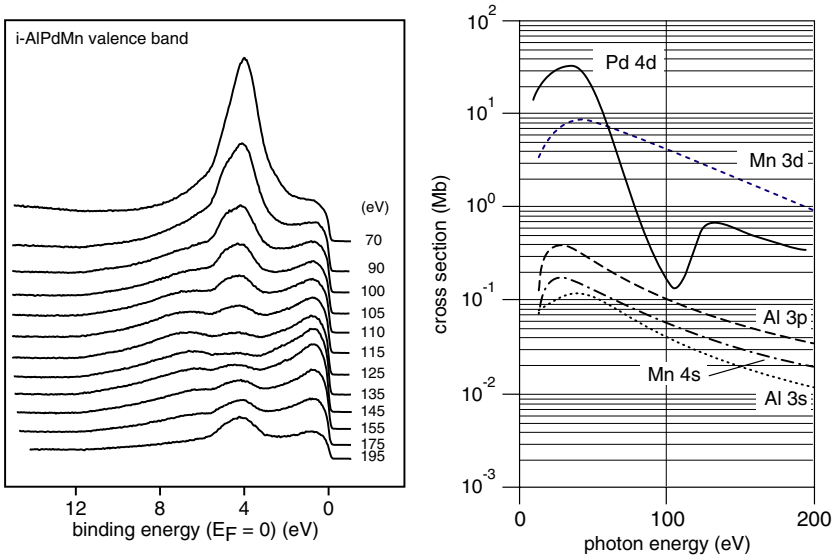

Figure 2. Left: series of normal emission spectra from a freshly cleaved i-Al–Pd–Mn sample, recorded at normal emission for photon energies from 70 to 195 eV. The peak which is strongly suppressed at higher photon energies is attributed to emission form the Pd 4d level. Right: atomic photoionization cross sections $\sigma(\hbar\omega)$ or the Al, Pd and Mn states, calculated within the Hartree–Fock–Slater scheme by Yeh and Lindau [30], showing the strong Cooper minimum in the Pd 4d line.

in the radial distribution of the wavefunction, while the Mn 3d states have none. This node in the Pd 4d wavefunction gives rise to the Cooper minimum [26] in the photoionization cross section that is well known for d states with main quantum number $n > 3$. The strength of this effect can be seen in the series of normal emission spectra from i-Al–Pd–Mn, recorded for photon energies from 70 to 195 eV in figure 2. The peak centred at 4 eV is strongly suppressed around photon energies of around 125 eV, before re-emerging at higher photon energies. The Cooper minimum has been used to obtain information on the electronic structure of metals, interfaces and alloys early on in photoemission with synchrotron radiation [27], for example to study disordered Au–Pd alloys [28]. The photon energy at which the minimum occurs has been found to be shifted with respect to the calculated value, lying around $h\nu = 140$ eV in the Au–Pd alloy study, and this shift has been ascribed to spatial distortions of the Pd 4d wavefunction in the Au–Pd alloy [29].

At around 125 eV the structure near the Fermi edge is enhanced. In fact, the line shape in this region appears quite different from that at lower photon energies. The atomic photoionization cross sections $\sigma(\hbar\omega)$ of the valence Al, Pd, and Mn states, calculated within the Hartree–Fock–Slater scheme by Yeh and Lindau [30] are shown on the right-hand side of figure 2. From these data it is clear that the Pd 4d and Mn 3d emission should dominate the valence level photoemission spectrum over other contributions by more than one order of magnitude in the photon energy region of figure 2. The interesting point is the strong difference in cross section between the Pd 4d and Mn 3d states. The former exhibits a strong maximum around 50–60 eV kinetic energy, followed by a steep decline by almost two orders of magnitude at around 110 eV, with a subsequent increase towards higher kinetic energies. This behaviour causes a difference in intensity from the Pd and Mn states that gives rise to the strong changes in the appearance of the spectra in figure 2.

Since the emission from the Pd 4d level is identified to be centred at about 4 eV below E_F, suggesting that there are no Pd 4d states near E_F, we conclude that the Mn 3d level with its d^5 occupancy contributes most to the emission near E_F. We will identify this contribution in resonant photoemission in section 3.2, and interpret contributions from the s valence states of Al, Pd, and Mn in section 3.3. The shape of the Pd 4d peak appears to have a broad doublet structure, which is evident in the spectrum at 90 eV, reminiscent of a spin–orbit-like splitting. Its Lorentzian-like shape, which is expected from the theory of such virtual bound states [21], appears to extend quite close towards the Fermi edge, since there is a pronounced line shape change from E_F down to about 3 eV as the Cooper minimum is approached. Under conditions where the Pd 4d contribution is suppressed, the spectrum near E_F is then representative of the d state contribution from Mn, for example at a photon energy of 125 eV. The valley caused by the decrease of the Pd peak extends to both the low and high binding energy sides. This enhances the contributions of the s–p states from Al, Pd and Mn, which in the respective bulk metals extend to binding energies up to about 11 eV. These are responsible for the slow rise towards the Pd peak from the side of higher binding energies. Beyond the Cooper minimum, the intensity in the Pd 3d region increases again, as expected from the trend in the cross section calculations, which predict a moderate increase beyond the minimum.

3.2. Resonant valence level photoemission in the region of the Mn L absorption edge

The assignment of the valence region to different atomic species can be put onto a more solid foundation, through the application of resonant photoemission. Here the ionization cross section of an outer-shell electron is enhanced as the excitation energy exceeds the threshold of an inner core level excitation. Resonant photoemission is widely used for the identification of specific contributions to the valence band; for a recent review, see [31]. The method is based on strong variations in the photoionization cross section at certain photon energies, which are due to the configuration mixing of two different states: (i) a continuum final state representing the outgoing photoelectron and the remaining photohole, and (ii) a discrete intermediate state populated by a dipole transition and decaying via an Auger process. Since the probability of transitions into the intermediate state varies dramatically when tuning the photon energy across a core level threshold, large variations of the cross section are obtained, known as Fano–Beutler resonances in atomic physics [32]. The Auger process involved represents an element-specific local probe, and thus the cross section variations are particularly useful to discriminate spectral contributions of different elements in the valence band photoemission spectra of compounds. This method has been previously applied to quasicrystals [13, 33, 34] to identify features in the valence bands of Al–Pd–Mn and Al–Cu–Fe quasicrystalline alloys. In these studies the 3p levels were used; however, these give rise, because of their more extended character, to weak resonantly enhanced structures, such that no distinction of the character of states contributing to specific regions of the valence band could be made. The use of deeper core levels such as the 2p lines induces a stronger resonant p–d transition, and thus clearer variations in the valence band emission as the 2p threshold is passed. The intermediate state for detecting manganese contributions is then the $2p^5 3d^6$ configuration. In view of the deep core levels involved and the generally low flux in this photon energy region, valence level photoemission is often hardly feasible. The high flux available on beamline 7 at ALS combined with an efficient analyser permits a recording of Mn-derived features upon crossing the Mn L edge (2p excitation) as seen from the data in figure 3, even though Mn only constitutes a minority species with 8.5% concentration in i-Al–Pd–Mn. The right-hand vertical spectrum in figure 3 shows the total electron yield signal as a function of photon energy, where the Mn $2p_{3/2}$ and $2p_{1/2}$ absorption lines are clearly visible. The bottom spectrum on the left-hand side is a valence

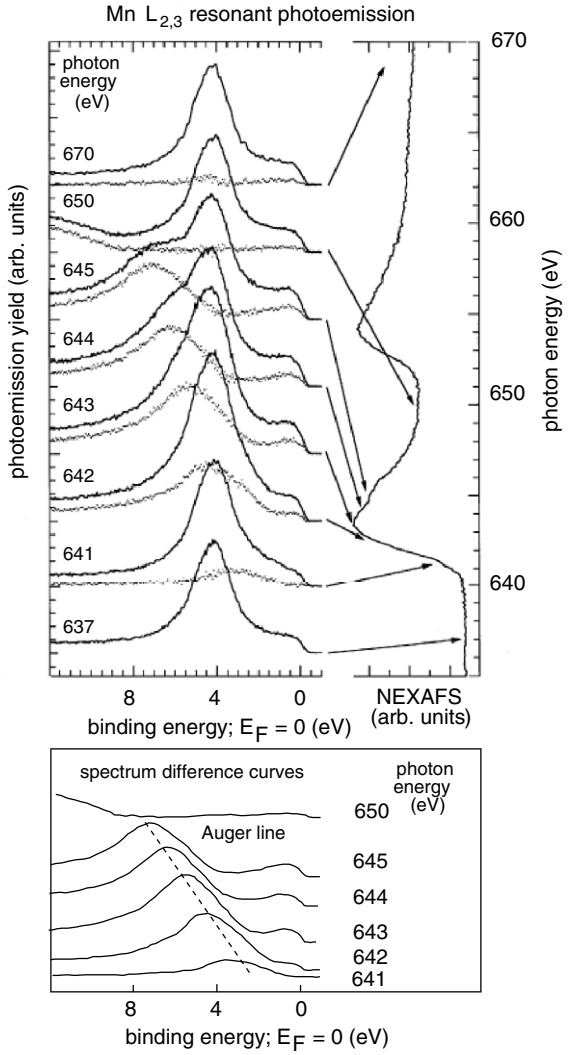

Figure 3. Set of (horizontal) valence level spectra from i-Al–Pd–Mn in the region of the Mn L threshold, plotted against the (vertical) absorption spectrum recorded in total electron yield against photon energy, with the Mn $2p_{3/2}$ and $2p_{1/2}$ absorption lines clearly visible. The dotted curves below each valence level spectrum correspond to the difference between each spectrum and the first, off-resonance one. The broad peak emerging near the Fermi energy at about 643 eV photon energy, which moves towards higher binding energy through the difference spectra with increasing photon energy, relates to the Auger transition associated with the excitation of the Mn 2p level.

level spectrum off-resonance, i.e. below the onset of the Mn 2p excitation, as indicated by the arrow. The valence level spectra above the bottom one are for different photon energies (solid lines), while the dotted curves below each valence level spectrum correspond to the difference between each spectrum and the first, off-resonance one. A broad peak is seen to be emerging near the Fermi energy, and to be moving towards higher binding energy through the difference spectra with increasing photon energy; this is the L_3 VV Auger transition associated with the excitation of the Mn 2p level. Important for our present purposes is the enhancement of the

region immediately below the Fermi edge, which is clearly observable in the spectra recorded at 642.5–645 eV photon energy, i.e. in the maximum of the Mn 2p absorption. It is largely absent for a photon energy of 650 eV, in the valley between the $2p_{3/2}$ and $2p_{1/2}$ excitation lines. From the difference spectrum at a photon energy of 646 eV it is obvious that the contribution of the manganese 3d electrons to the Al–Pd–Mn valence band occurs in the region from E_F up to about 3 eV binding energy, with a peak at about 1 eV below E_F.

3.3. Analysis of Pd 3d core level line shape asymmetry

An important aspect of quasicrystal electronic structure investigations has been the identification of the density of states near E_F, and the so-called pseudogap [23]. Whereas we have utilized photoionization cross section variations and resonant photoemission for this purpose above, photoemission offers another means of detecting contributions from different atomic species to the density of states near E_F through a line shape analysis of the core levels of the constituent atoms. In an earlier investigation, we have addressed the issue of the quasigap through a joint analysis of line shape of the Al 2p core level, and valence band photoemission [11]. Here we analyse the differences in line shape of the Pd 3d and Mn 2p levels by comparing the elemental metal spectrum with that from an i-Al–Pd–Mn quasicrystal. Core level lines from metals exhibit a specific asymmetry towards higher binding energies, which arises from low-energy excitations of the Fermi sea of conduction electrons, in the process of the screening of the photoinduced core hole. Shevchik [35] has shown how the asymmetry of the core level lines may change upon alloying, and how such changes may be interpreted in terms of differences in the valence level electronic structure. Here we apply such an analysis, supported by a quantitative evaluation of the line shape asymmetries, to the case of quasicrystalline i-Al–Pd–Mn. Upon creation of a core hole in a metal, a variety of excitation processes may take place as a reaction [36]. The positively charged ion contracts and sets up collective excitations of the electrons (plasmons), vibrational excitations of the neighboring nuclei (phonons), and excites electrons from near the Fermi energy into unfilled states to screen the positive charge, producing electron–hole pairs. It is the understanding of this latter process which marked a major milestone in the theory of photoemission, and we will try to utilize it here for an analysis of core level line shapes and their connection with the s–p density of states near E_F. A short summary of the origin of line shape asymmetry is given in the appendix.

Bearing these basic ideas in mind, let us examine the core level line shapes of the constituent atoms in i-Al–Pd–Mn. We rely here on a comparison of core level lines in the pure metal and the quasicrystalline alloy, such that atomic parameters such as the phase shifts mentioned above are not likely to be much different. In a previous publication, we have analysed the shape of the Al 2p line [11] in terms of a Doniach–Sunjic function, and for surface-sensitive conditions found a value for α very close to that for clean Al metal. For more bulk-sensitive conditions a decrease of α was observed, which was interpreted as indicating that metallicity was restricted to the surface region. The situation is entirely different for the Pd 3d core level, in that a large difference in asymmetry is observed between the quasicrystalline Al–Pd–Mn and the metallic Pd phase. The spectra from i-Al–Pd–Mn are shown for several photon energies at the bottom of figure 4, recorded at an energy resolution of about 100 meV. The top spectrum was recorded using an Al Kα laboratory x-ray source, from a polycrystalline sample of pure Pd cleaned by ion bombardment, at a resolution of about 0.75 eV. While the difference in resolution clearly affects the observed line width, it is quite obvious even without line shape analysis that the Pd lines from the Al–Pd–Mn sample are quite symmetric, compared to the pronounced asymmetry of the line from the metallic sample. In order to quantify this information, we

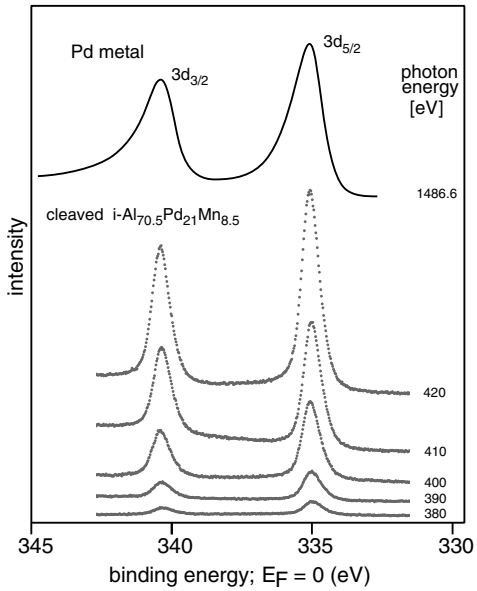

Figure 4. Pd 3d core level spectra. Top: pure Pd metal, recorded with monochromatized Al Kα laboratory source radiation. Lower spectra: Pd 3d lines from a freshly cleaved i-Al–Pd–Mn quasicrystal recorded with synchrotron radiation at the photon energies indicated (see text).

have subjected both data sets to a line shape analysis based on a nonlinear least-squares fitting routine using the Levenberg–Marquardt algorithm [37]. The model function is a spin–orbit split Doniach–Sunjic function, convoluted with a Gaussian to model instrumental, thermal, and inhomogeneous broadening, and a third-order polynomial background plus a Shirley-type step function [38] to model the inelastically scattered electrons. The results of this line shape analysis are shown in figure 5, together with the separate components of the model function. The residuum is shown beneath each spectrum, scaled to the statistical error which is given by the upper and lower straight lines. It shows that the model function gives a good description of the experimental data in both cases, with only small systematic deviations from the zero line.

The results of the line shape analysis yield the following results. For pure Pd metal, the lifetime broadening γ is 210 meV, and the asymmetry parameter α is 0.18, somewhat lower than the value derived from a study using monochromatized Al Kα radiation by Wertheim and Citrin [36] for pure Pd. This line shape analysis is made difficult by a possible influence of low-lying excitations on the high binding energy side. The Pd 3d line shape from i-Al–Pd–Mn is best described by a lifetime broadening of 171 meV, and an asymmetry parameter of $\alpha = 0.03$ with a confidence interval of 0.02, i.e. very close to zero. This strong decrease in the asymmetry parameter shows the virtual absence of Pd-derived valence states in the vicinity of E_F. Not only does this refer to the Pd 4d states, which give rise to the peak located about 4 eV below E_F and are therefore unlikely to contribute in any case, but also the s–p-derived states which cannot be separated from the contributions of Al and Mn states in the vicinity of E_F by direct observation of the valence level spectrum. The line shape of the Pd 3d core level reveals the absence of these states in an indirect yet straightforward manner, a point that is discussed in more detail in connection with the contributions of the Mn states to the region around E_F below. Our data agree with those by Fournée *et al* [9], who find a reduction of α from 0.21 in metallic Pd to 0.05 in the fractured or sputter-annealed i-Al–Pd–Mn, recorded with Mg Kα radiation.

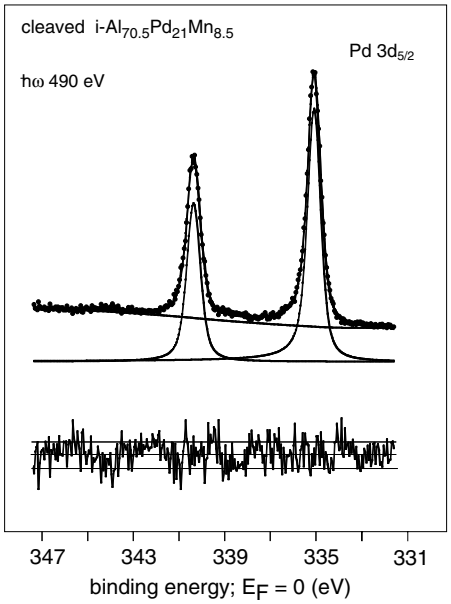

Figure 5. Analysis of the Pd 3d core level line shape from a freshly cleaved i-Al–Pd–Mn sample, recorded at a photon energy of 490 eV, using the procedure described in the text. The data below the spectrum give the residual, with the upper and lower lines indicating the scatter expected from the counting statistics.

3.4. Analysis of Mn 2p core level line shape asymmetry

A similar analysis may be applied to the Mn 2p core level line. Data for this line from i-Al–Pd–Mn are shown in figure 6 (only the Mn $2p_{3/2}$ is displayed), together with the results from a fit using again the Doniach–Sunjic line shape, as for the Pd data in figure 5. The spectrum was recorded well above threshold, but in view of its minority species character the peak resides on a fairly large sloping background; however, the background shape is almost linear in this region such that a disturbing influence on the derivation of the line shape parameters is unlikely. The lifetime broadening γ is 151 meV, and the asymmetry parameter turns out to be $\alpha = 0.135$. Fournée *et al*, in a recent core level photoemission study of a large number of quasicrystals [10], found asymmetries for the M 2p line in elemental Mn metal ($\alpha = 0.46$), for cubic $Al_{57}Pd_{36}Mn_7$ ($\alpha = 0.43$), for the cubic surface structure of i-$Al_{72}Pd_{19.5}Mn_{8.5}$ ($\alpha = 0.43$), and for the i-$Al_{72}Pd_{19.5}Mn_{8.5}$ quasicrystal prepared by fracturing ($\alpha = 0.18$). This latter value comes close to our result above. However, the evaluation of Mn 2p core level line shapes may not be without pitfalls. Sandell *et al*, in a recent study of thin Mn films on Pd(100), found that the main Mn 2p line is accompanied by a satellite line at about 1 eV higher binding energy [39]. This satellite showed intensity variations with the local structure of the Mn atom environment. Both the main line and the satellite were assigned to a $2p^5 3d^6$ final state. The occurrence of main line and satellite was attributed to differences in final state screening, being caused by 'local screening' through the palladium 4d-derived states near the Fermi level, leading to the main line, and 'nonlocal screening' from the surrounding $MnPd_x$ units, leading to the satellite. The situation in Al–Pd–Mn is different from that of the Mn–Pd bimetallic system since the Pd 4d states do not extend up to the Fermi level as shown above. Thus if a local screening process were to give rise to the main line in Al–Pd–Mn it would have to occur through aluminium-derived s–p states near E_F. The occurrence of such a satellite feature as

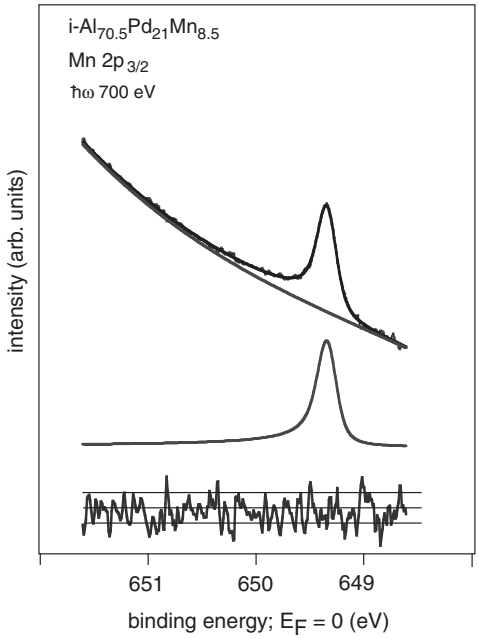

Figure 6. Analysis of the Mn 2p core level line shape from a freshly cleaved i-Al–Pd–Mn sample, recorded at a photon energy of 700 eV, using the procedure described in the text.

a function of local environment in the quasicrystalline alloy may then mimic a large value in α that is not related to the ground state density of valence states. For the moment, this question must remain unanswered. The asymmetry parameter in the AlMn alloy, derived from the 3s level using monochromatized Al Kα radiation, numerically extracted from the literature and analysed within our fitting routine, is $\alpha = 0.24$ [40], considerably larger than the value reported here for Al–Pd–Mn, suggesting that the density of states in this alloy may be lower than in bulk Mn but not as low as in the quasicrystal.

To what extent can the changes in asymmetry parameter be related to the specific electronic structure of a quasicrystal, i.e. the presence of a pseudogap? In a systematic study of several different quasicrystals and approximants, Fournée *et al* have recently compared the Mn 2p, Ni 2p and Co 2p lines with those of the respective bulk metals [10]. They find a systematic trend such that the asymmetry parameters are smallest in the quasicrystalline phases. This is attributed to the reduction in the density of states at E_F by the pseudogap. They also find an increasing asymmetry with enhanced surface sensitivity [9]. A similar effect had been seen in the Al 2p line in cleaved i-Al–Pd–Mn by Neuhold *et al* [11], indicating an enhanced metallic character in the surface of the quasicrystal. The trend in the data of Fournée *et al* renders it implausible to assign such trends to a dilution of the Mn atoms in the alloy matrix. However, the interpretation of a low value of α in the quasicrystalline phase, in terms of the reduction of the density of states through the occurrence of a pseudogap at E_F, is also not without problems. The reduction in the density of states below E_F through the pseudogap covers an energy region of a few hundred meV, depending on the function that is used to model the shape of the pseudogap. Stadnik *et al* [8], in their high-resolution photoemission study of Al–Cu–Fe, Al–Pd–Mn, and Al–Pd–Re quasicrystals, analyse their data on the basis of a Lorentzian shape of the pseudogap, and find the width of the pseudogap to be between 0.22

and 0.34 eV. From the discussion of the assumptions on which the Doniach–Sunjic line shape is based, an interpretation of the asymmetry in terms of a single parameter for such cases is of course problematic. The large reduction in asymmetry in the Pd 3d line clearly suggests that the levels involved in screening are removed from E_F by a large amount. The resonant photoemission data in figure 3, and the enhancement of the valence band region near E_F in the spectra of figure 2, demonstrate that the Mn 3d states extend very close up to the Fermi level. Hensch *et al* [41] have suggested that the Mn 3d band is shifted downwards by 0.9 eV from E_F, through an analysis of CVV Auger data. While the centre of gravity of the Mn 3d band may be shifted downwards by this amount, the data in figures 2 and 3 nevertheless show that it actually does extend up to E_F.

4. Summary

The data presented above show how core and valence level photoemission and photoabsorption from complex alloy phases such as $Al_{70.5}Pd_{21}Mn_{8.5}$ can be used to elucidate their electronic structure in terms of contributions from the different constituents to the valence levels, and the question of the magnitude of the density of states at the Fermi level. Cross section effects are useful to enhance or suppress contributions from different species, such as the Pd 4d levels, and this has helped to identify the energy range of the manganese-derived levels in the valence band. Photoabsorption in the region of the Mn L edge has been used to provide an alternative way to identify this contribution. As for the analysis of the line shape of the different core levels from the alloys constituents, a fingerprint-like way to distinguish between the environment of the respective metal atom, through strong changes in the asymmetry parameter α, as shown for several quasicrystals and approximants by Fournée *et al* [9, 10] as well as here, can be helpful in determining qualitative changes in the reduction of the density of states. This can be used for the analysis of different quasicrystalline and crystalline phases induced by the preparation process (such as sputtering and annealing) that occur in surface studies of quasicrystals. A detailed quantitative analysis of this parameter in such terms is, however, precluded by the complexity of the process involved in the excitations that lead to the asymmetry. Moreover, excitations accompanying the core level excitation might even complicate this topic even more. Thus a quantitative determination of the depth and width of the pseudogap through this method is not likely to succeed.

Acknowledgments

KH, WTh, SRB, and JJP acknowledge the excellent support of the staff of the Advanced Light Source. JJP also acknowledges support from the Deutsche Forschungsgemeinschaft through project Pa661/2-1. KH acknowledges support from the Network of Excellence ‘Complex Metallic Alloys’, contract NMP3-CT-2005-500145 from the European Union.

Appendix. Origin of core level photoemission line shape asymmetry

The many-body nature of physical processes involved in x-ray absorption and emission was described by Mahan [42], who predicted enhanced absorption above the threshold for excitations of a core hole into an unoccupied state; this can be thought of as an excitonic process. Anderson [43] noted that an additional process must be considered in the core hole screening process, since the initial state wavefunction of each electron in the conduction band is slightly modified in the core-ionized state. The transition matrix element must contain not only the overlap of the initial and final state of the core hole that is excited into the conduction band, but also the overlap of all the other wavefunctions of the many body system. This severely

reduces the transition strength to states near E_F. A mathematical solution to the absorption edge problem, containing both the Mahan enhancement and the Anderson suppression, was given by Nozières and de Dominicis [44]. They showed that the absorption coefficient $A(E)$ near threshold has the frequency dependence

$$A(E) = \left(\frac{1}{E}\right)^{\beta_l} \tag{A.1}$$

where E is the energy above threshold ($E = 0$ at threshold). The screening effects are contained in the threshold exponents β_l through

$$\beta_l = \frac{2\delta_l}{\pi} - \alpha \tag{A.2}$$

where

$$\alpha = 2\sum_l (2l+1)\left(\frac{\delta_l}{\pi}\right). \tag{A.3}$$

Here l is the orbital quantum number. The first term in (A.2) corresponds to Mahan's excitonic enhancement, while the second, the asymmetry parameter α, accounts for Anderson' suppression. The presence of the 'impurity', i.e. the core-ionized atom, on the wavefunctions of the conduction electrons scattered from the ion, is described by the Friedel phase shifts δ_l which are used in the theoretical description of transition metal impurities [45]. These phase shifts are constrained by the Friedel sum rule:

$$Z = 2\sum_l (2l+1)\left(\frac{\delta_l}{\pi}\right) \tag{A.4}$$

where the screening charge Z is unity for x-ray absorption, emission, and photoemission. Depending on the sign of the scattering phase shifts, β_l may be positive or negative, and this strongly affects the shape of the edge in x-ray absorption.

In a photoemission experiment, a fast photoelectron with an energy well above the conduction band is created, such that the excitonic Mahan term in (A.2) does not contribute. We can therefore concentrate on a discussion of the second term α, which may be deduced directly from the core level photoemission line shape.

The essential physics of electron–hole response in the x-ray photoemission spectrum from a metal can be grasped in a perturbational approach by Hopfield [46], who considered the effect of a suddenly applied potential on a Fermi gas. The short-range part of the potential is assumed to have constant matrix elements V_0 between s states close to E_F. Perturbation theory then shows that the transition probability for excitations of energy E is proportional to V_0^2/E^2. For small excitations the density of electron–hole pairs is $N_0^2 E$, where N_0 is the density of states at E_F. The average number of electron–hole pairs is then given by

$$\bar{n} = \int_0^{E_c} \left(\frac{V_0^2}{E^2}\right)(N_0^2 E)\,\mathrm{d}E = V_0^2 N_0^2 \int_0^{E_c} \frac{\mathrm{d}E}{E} \tag{A.5}$$

where E_c is an energy cutoff. There is thus a logarithmic divergence as E approaches zero, i.e. an infrared catastrophe. For a situation where $V_0^2 N_0^2$ is a constant B in the region $0\langle E\rangle E_c$, the spectrum of excitations has a simple solution:

$$f(E) = \left(\frac{1}{E}\right)^{1-B}. \tag{A.6}$$

This is formally similar to the description of the screening process by Anderson, and permits a connection between the screening charges and the scattering phase shifts. The expression

of the total screening charge can be broken down into the screening charges for each orbital quantum number l through the Friedel sum rule (A.4), which in terms of the screening charges q_l becomes

$$\sum q_l = \sum 2(2l+1)\left(\frac{\delta_l}{\pi}\right). \tag{A.7}$$

We can then combine this with the expression for the asymmetry parameter α to obtain a direct connection between the phase shifts and the screening charges:

$$\alpha = \sum \frac{q_l}{2(2l+1)}. \tag{A.8}$$

Thus since α contains the squares of the screening charges, it is possible to interpret the exponent $(1-B)$ in equation (A.6) in a simple physical way. A weak, attractive potential acting on the electrons in the conduction band lowers their energy with respect to the Fermi level, such that an additional charge V_0N_0 can be accommodated. However, this direct connection between the screening charges and the asymmetry parameter depends on the assumption of a constant density of states over an appreciable energy range near E_F. The influence of different shapes of the density of states near E_F on the shape of the core level line was calculated numerically by Wertheim and Walker [47], showing that a constant DOS and one which follows the free-electron-like case (i.e. a $\sqrt{E}$ behaviour) are very similar. Other shapes, in particular a finite range of the DOS above E_F, were found to have a strong influence on the line shape.

A useful result, which has found a widespread application in core level photoemission, is the description of the asymmetric line shape in a closed form by Doniach and Sunjiç [48]. They combine the power law dependence with a finite hole state lifetime γ to arrive at a spectral function $f(E)$:

$$f(E) = \frac{\Gamma(1-\alpha)\cos[\pi\alpha/2 + (1-\alpha)\arctan(E/\gamma)]}{(E^2+\gamma^2)^{(1-\alpha)/2}} \tag{A.9}$$

where Γ is the gamma function. For $\alpha = 0$ $f(E)$ is a Lorentzian, and for $E/\gamma \gg 1$ the power law form is obtained. The Doniach–Sunjic line shape describes the asymmetry of core level lines reasonably well in many cases, although there are some serious discrepancies in the case of some transition metals. Pd is a case in point; here a description assuming an almost filled rectangular conduction band is much better [47]. As for the simple metals, the magnitudes of α for the cases of Na, Mg and Al agrees well with a reasoning on the basis of the principles laid out above, taking into account the relative magnitude of the phase shifts, with α being largest for Na with a wide unoccupied s band. The unoccupied density of states for Mg, and even more so for Al, is more p-like and hence α is smaller. However, in general the dependence of the asymmetry parameter α on the screening charges and thus on the phase shifts (equations (A.7) and (A.8)) renders a prediction of this parameter difficult, and indeed inhibits an interpretation of the states involved in core hole screening, such that only upper and lower limits for α have been identified in a few cases [49].

References

[1] DiVicenzo D P and Steinhardt P J 1991 *Quasicrystals—The State of the Art, Directions in Condensed Matter Physics* vol 11 (Singapore: World Scientific)

[2] Janot C 1994 *Quasicrystals—a Primer* (Oxford: Oxford University Press)

[3] Goldman A I, Sordelet D J, Thiel P A and Dubois J M 1997 *New Horizons in Quasicrystals: Research and Applications* (Singapore: World Scientific)

[4] Stadnik Z M 1999 *Physical Properties of Quasicrystals* (*Springer Series in Solid State Sciences*) vol 126 (Berlin: Springer)

[5] Kevan S D 1992 *Angle-Resolved Photoemission, Studies in Surface Science and Catalysis* vol 74 (Amsterdam: Elsevier)
[6] Horn K and Scheffler M 2000 *Handbook of Surface Science* vol II (Amsterdam: Elsevier Science)
[7] Matsubara H, Ogawa S, Kinoshita T, Kishi K, Takeuchi S, Kimura K and Suga S 1991 *Japan. J. Appl. Phys.* A **30** L389
[8] Stadnik Z M, Purdie D, Garnier M, Baer Y, Tsai A-P, Inoue A, Edagawa K and Takeuchi S 1996 *Phys. Rev. Lett.* **77** 1777
[9] Fournée V, Pinhero P J, Anderegg J W, Lograsso T A, Ross A R, Canfield P C, Fisher I R and Thiel P A 2000 *Phys. Rev.* B **62** 14049
[10] Fournée V, Ross A R, Lograsso T A and Thiel P A 2002 *J. Phys.: Condens. Matter* **14** 2691
Fournée V, Anderegg J W, Ross A R, Lograsso T A, Evans J W and Thiel P A 2003 *Surf. Sci.* **537** 5
[11] Neuhold G, Barman S R, Horn K, Theis W, Ebert P and Urban K 1998 *Phys. Rev.* B **58** 754
[12] Davydov D N, Mayou D, Berger C, Gignoux C, Neumann A, Jansen A G M and Wyder P 1996 *Phys. Rev. Lett.* **77** 3173
[13] Zhang G W, Stadnik Z M, Tsai A-P and Inoue A 1994 *Phys. Lett.* A **186** 345
[14] Wu X, Kycia S W, Olson C G, Benning P J, Goldman A I and Lynch D W 1995 *Phys. Rev. Lett.* **75** 4540
[15] Rotenberg E, Theis W, Horn K and Gille P 2000 *Nature* **406** 602
[16] Jenks C J, Chang S L, Anderegg J, Thiel P A and Lynch D W 1996 *Phys. Rev.* B **54** 6301
[17] Gierer M, van Hove M A, Goldman A I, Shen Z, Chang S-L, Jenks C J, Zhang C-M and Thiel P A 1997 *Phys. Rev. Lett.* **78** 467
[18] Naumovic D, Aebi P, Schlapbach L and Beeli C 1997 *New Horizons in Quasicrystals* ed A I Goldman, D J Sordelet, P A Thiel and J M Dubois (Singapore: World Scientific)
[19] Zheng J-C, Huan C H A, Wee A T S, Van Hove M A, Fadley C S, Shi F J, Rotenberg E, Barman S R, Paggel J J, Horn K, Ebert Ph and Urban K 2004 *Phys. Rev.* B **69** 134107
[20] Raether H 1980 *Excitation of Plasmons and Interband Transitions by Electrons* (Berlin: Springer)
[21] Hüfner S 1993 *Photoelectron Spectroscopy* (Berlin: Springer)
[22] Belin E, Dankhazi Z, Sadoc A and Dubois J-M 1994 *J. Phys.: Condens. Matter* **6** 8771
[23] Kraijci M, Windisch M, Hafner J, Kresse G and Mihalkoviç M 1995 *Phys. Rev.* B **51** 17355
[24] Zijlstra E S and Janssen T 2000 *Phys. Rev.* B **61** 3377
[25] Zijlstra E S and Jansen T 2000 *Europhys. Lett.* **52** 578
[26] Cooper J W 1962 *Phys. Rev.* **128** 681
[27] Abbati I, Braicovich L, Rossi G, Lindau I, del Pennino U and Nannarone S 1983 *Phys. Rev. Lett.* **50** 1799
[28] Nahm T-U *et al* 1998 *Phys. Rev.* B **58** 9817
[29] D'Addato S, Brooks N J, Thornton J M C, Unsworth P, Weightman P, Duò L and Sancrotti M 1996 *J. Phys.: Condens. Matter* **8** 1413
[30] Yeh J J and Lindau I 1985 *At. Data Nucl. Data Tables* **32** 1
[31] Laubschat C 1998 *J. Electron Spectrosc. Relat. Phenom.* **96** 127
[32] Fano U 1961 *Phys. Rev.* **124** 1866
[33] Stadnik Z M and Stroink G 1993 *Phys. Rev.* B **47** 100
[34] Mori M, Kamiya K, Matsuo S, Ishimasa T, Nakano H, Fujimoto H and Inokuchi H 1992 *J. Phys.: Condens. Matter* **4** L157
[35] Shevchik N J 1974 *Phys. Rev. Lett.* **33** 1336
[36] Wertheim G K and Citrin P H 1978 *Photoemission in Solids* ed M Cardona and L Ley (Berlin: Springer)
[37] Theis W 1992 *PhD Thesis* Freie Universität Berlin
[38] Shirley D A 1972 *Phys. Rev.* B **5** 4709
[39] Sandell A and Jaworowski A J 2004 *J. Electron Spectrosc. Relat. Phenom.* **135** 7
[40] Moulder J F, Stickle W F, Sobol P E and Bomben K D 1992 *Handbook of X-ray Photoelectron Spectroscopy* (Eden Prairie, MN: Perkin-Elmer Corporation)
[41] Hensch A, Rossner B, Bolliger B and Erbudak M 2001 *Surf. Sci.* **489** 169
[42] Mahan G D 1967 *Phys. Rev.* **163** 612
[43] Anderson P W 1967 *Phys. Rev. Lett.* **18** 1049
[44] Nozieres P and De Dominicis C T 1969 *Phys. Rev.* **178** 1049
[45] Harrison W A 1989 *Electronic Structure and the Properties of Solids* (New York: Dover)
[46] Hopfield J J 1969 *Comments Solid State Phys.* **2** 40
[47] Wertheim G K and Walker L R 1976 *J. Phys. F: Met. Phys.* **6** 2297
[48] Doniach S B and Sunjic M 1970 *J. Phys. C: Solid State Phys.* **3** 285
[49] Hüfner S and Wertheim G K 1978 *Photoemission in Solids* ed M Cardona and L Ley (Berlin: Springer)